Laminar convective heat transfer characteristic of Al_2O_3/water nanofluid in a circular microchannel

K Trinavee[1, 3], T K Gogoi[1] and M Pandey[2]
[1]Department of Mechanical Engineering, Tezpur University, Tezpur, Assam, India
[2]Department of Mechanical Engineering, IIT Guwahati, Assam, India

[3]kumari.trinavee779@gmail.com

Abstract. In this study, laminar convective heat transfer characteristics Al_2O_3/water nanofluid in a circular microchannel is investigated using a two-phase (discrete phase) model. The computational fluid dynamic code FLUENT (ANSYS) is employed to solve the coupled momentum and energy equations with the boundary conditions of uniform wall heat flux and velocity at channel inlet. Detail analysis is done showing variation of wall temperature, fluid bulk mean temperature, heat transfer coefficient, Nusselt number, shear stress, friction, pressure drop, entropy generation etc. along the microchannel at two particle volume concentrations (1% and 4%) of the nanofluid. Comparison of results is provided between base and nanofluid and also for two cases, one with constant property and the other with variable temperature thermal conductivity and viscosity. Results show that heat transfer is enhanced in case of the nanofluid with low entropy generation and the heat transfer parameters increase with increase in nanoparticle volume concentration and Reynolds number. However, use of nanofluid also causes increase in pressure drop and shear stress. A comparison of the constant and variable property model showed that heat transfer is further enhanced; entropy, shear stress and pressure drop further decrease when temperature dependent properties of the nanofluid are considered instead of constant properties.

1. Introduction

Use of nanofluids in heat exchangers and cooling devices has received significant research interest in the recent past. Many experimental studies have been carried out to evaluate convective heat transfer characteristics of nanofluids in tubes [1-3], microsystem with single microchannel [4], multiple parallel rectangular micro-channels [5, 6] and wide rectangular microchannel [7]. Al_2O_3/water in various volume concentrations were considered in the above studies under laminar flow condition except in in Hozzat et al. [3] where the study was done under turbulent flow conditions considering Al_2O_3, CuO, and TiO_2 nanoparticles and carboxymethyl cellulose (non-Newtonian base fluid). The above studies have reported heat transfer enhancement with nanofluids with higher concentration in the base fluid. It was also observed that the heat transfer enhancement is more in the entrance region compared to the fully developed region [1, 5].

Simultaneously numerical analyses have also been done to predict heat transfer behavior of nanofluids under laminar [7-16] and turbulent flow conditions [17-19]. Some studies [8, 9, 17] used single phase method while some others [7, 12, 14, 19] employed two-phase method for modeling nanofluids. The single phase method, where the nanofluid is considered as homogeneous mixture of nanoparticles, is simple and computationally efficient. In the two-phase method, the nanoparticles and the base fluid are considered as solid and liquid with different velocity and temperatures. Bianco et al. [12] used both single-phase and two-phase methods considering constant and temperature dependent properties of the Al_2O_3/water nanofluid. Kalteh et al. [14] investigated laminar forced convection heat

transfer of Cu/water nanofluid inside an isothermally heated parallel plate microchannel using single and two phase models. There is another method based on Boltzmann theory that considers nanoconvection due to Brownian motion and particle collision [10, 11, 20].

The numerical studies discussed above were basically conducted on circular tubes [8, 12, 17-19], rectangular micro channels [9, 10], trapezoidal channel [11], parallel disc [13], parallel plate microchannel [14, 15] and wide rectangular channel [7] etc. The heat transfer performance of a system varies with the shape and size of the coolant flow channel. Theoretical analyses on a circular microchannel heat sink using nanofluids are not many. Sohel et al. [21] made a comparative analysis in a circular microchannel using Al_2O_3/water, TiO_2/water and CuO/water nanofluids under laminar flow condition. Sohel et al. [22] in another study considered circular microchannels and minichannels to analyze entropy generation rate under turbulent flow condition using Cu, Al_2O_3 nanoparticles and water, ethylene glycol base fluids. Zhang et al. [23] presented an experimental study using Al_2O_3/water nanofluid with 0.25%, 0.51% and 0.77% volume concentrations through a circular microchannel of 0.5 mm inner diameter. In this study, laminar convection of Al_2O_3/water nanofluid in a circular microchannel with 1% and 4% particle volume concentrations is numerically investigated. Ansys (Fluent) 14.0 version is used to solve the problem. Both constant and temperature dependent thermophysical properties of nanofluid are taken into consideration and a comparative analysis is provided with complete details showing variation of heat transfer, entropy generation and flow parameters such pressure drop, friction and shear stress etc.

2. Mathematical modeling

The geometry of the circular microchannel is shown in Figure 1. It is assumed that Al_2O_3/water nanofluid is incompressible and its flow through the microchannel is developing, steady and laminar. Al_2O_3 particles are spherical with 38 nm diameter. Due to symmetry, only the upper half of the channel is considered to save the computational time. A two phase model [12] is employed to analyze the flow and heat transfer problem of nanofluid in the circular microchannel.

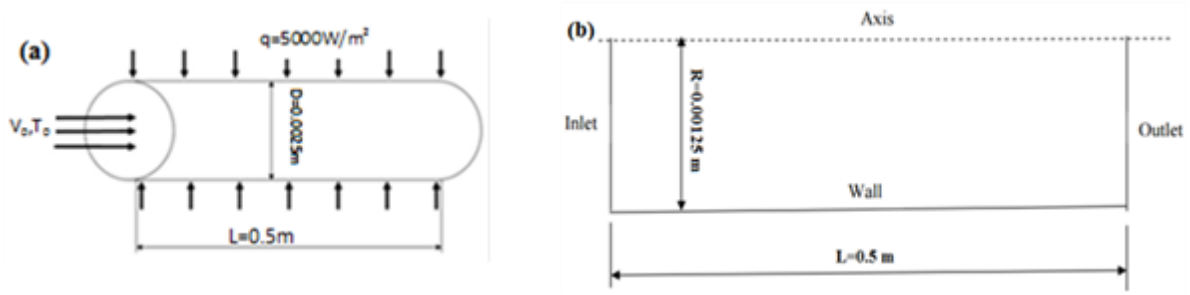

Figure 1. (a) Geometry of the circular microchannel (b) computational domain

2.1. Governing equations

The steady-state governing equations for the Eulerian-Lagrangian discrete two phase model are expressed as follows [12].

Continuity equation: $$\nabla.\left(\rho\vec{V}\right)=0 \quad (1)$$

Momentum equation: $$\nabla.\left(\rho\vec{V}\vec{V}\right)=-\nabla P+\nabla.\left(\mu\nabla\vec{V}\right)+S_m \quad (2)$$

Energy equation: $$\nabla.\left(\rho\vec{V}C_pT\right)=\nabla.\left(\lambda\nabla T\right)+S_e \quad (3)$$

Particle momentum and energy equations in Lagrangian form are as follows.

$$\frac{d\vec{V}_p}{dt} = F_D\left(\vec{V} - \vec{V}_p\right) + \frac{\vec{g}\left(\rho_p - \rho\right)}{\rho_p} + \vec{F} \quad (4)$$

$$\rho_p C_p \frac{dT_p}{dt} = \frac{6h}{d_p}\left(T - T_p\right) \quad (5)$$

$\vec{V}_p$ and T_p in equations (4) and (5) are the nanoparticle velocity and temperature respectively. ρ_p is the density and d_p is the diameter of the nanoparticles. Eq. (4) is the force balance equation for a particle immersed in the fluid and $\vec{F}$ in Eq. (4) accounts for additional forces due to rotation of reference frame, thermophoretic force, Brownian force etc. The gravity term in Eq. (4) and additional forces '$\vec{F}$' are however neglected in this analysis. F_D is the drag coefficient defined according to Stokes' law. Details about the calculation procedure of F_D is highlighted in Ref. [12]. In Eq. (5), h is the heat transfer coefficient, ρ and T refer to fluid density and temperature respectively. For the details including the source/sink terms (S_m and S_e) in Eq. (2) and Eq. (3), one can refer to the article in Ref. [12].

2.2. Boundary conditions

At the channel inlet, uniform axial velocity, V_0, and temperature, $T_0 = 293$ K, are assumed. Pressure outlet condition is specified at the channel exit. On the channel wall, the no-slip condition and uniform heat flux of 5000 W/m^2 are imposed.

2.3. Thermophysical Properties of the Nanofluids

The thermophysical properties of Al_2O_3 particles and base fluid are as follows [2, 12].

$\rho_p = 3880\ \text{kg/m}^3;\ Cp_p = 733\ \text{J/kgK};\ k_p = 36\ \text{W/mK}$

$\rho_{\text{bf}} = 998.2\ \text{kg/m}^3;\quad Cp_{bf} = 4182\ \text{J/kgK};\ k_{bf} = 0.597\ \text{W/mK};\ \mu_{\text{bf}} = 9.93\text{x}10^{-4}\ \text{kg/ms}$

Case1: Constant property model

Density: $\rho_{nf} = (1-\phi)\rho_{bf} + \phi\rho_p$ (6)

Specific heat: $Cp_{nf} = (1-\phi)Cp_{bf} + \phi Cp_p$ (7)

In this case, viscosity and thermal conductivity of the nanofluid is a function of T_0 only.

Dynamic viscosity: $\phi = 1\% \rightarrow \mu_{nf} = 3.4\times10^{-2} - 1.975\times10^{-4}T_0 + 2.912\times10^{-7}{T_0}^2$ (8)

$\phi = 4\% \rightarrow \mu_{nf} = 4.051\times10^{-2} - 2.353\times10^{-4}T_0 + 3.475\times10^{-7}{T_0}^2$ (9)

Thermal conductivity: $\phi = 1\% \rightarrow k_{nf} = 0.003352T_0 - 0.3708$ (10)

$\phi = 4\% \rightarrow k_{nf} = 0.004961T_0 - 0.8078$ (11)

Case 2: Temperature dependent property model

Density and specific heats are same with constant property model. However, viscosity and thermal conductivity vary with temperature in this case. Temperature dependent viscosity and thermal conductivity of nanofluid with different concentration are expressed as follows [12, 15].

Dynamic viscosity: $\phi = 1\% \rightarrow \mu_{nf} = 3.4\times10^{-2} - 1.975\times10^{-4}T + 2.912\times10^{-7}T^2$ (12)

$\phi = 4\% \rightarrow \mu_{nf} = 4.051\times10^{-2} - 2.353\times10^{-4}T + 3.475\times10^{-7}T^2$ (13)

Thermal conductivity: $\phi = 1\% \rightarrow k_{nf} = 0.003352T - 0.3708$ (14)

$\phi = 4\% \rightarrow k_{nf} = 0.004961T - 0.8078$ (15)

The viscosity and thermal conductivity of base fluid are also considered temperature dependent in the second case [12, 15].

$$\mu_{bf} = 7.57\times10^{-2} - 6.37\times10^{-4}T + 1.80\times10^{-6}T^2 - 1.73\times10^{-9}T^3 \quad (16)$$

$$k_{bf} = -1.13 + 9.71\times10^{-3}T - 1.31\times10^{-3}T^2 \quad (17)$$

2.4 Numerical method

Ansys fluent [24] version 14.0 was used to solve the present problem using a control volume approach. A second order upwind method was used for solving the momentum and energy equations. Pressure and velocity were coupled using Semi Implicit Method for Pressure Linked Equations (SIMPLE) algorithm. The convergence criteria was set to 10^{-6}. Three different non-uniform grids were considered to check grid independency of the numerical results. The non-uniform grid 500x50 was found acceptable. Grid independency was achieved as the wall temperature obtained with this grid size was almost the same with the non-uniform grid 700x60 (Refer Figure 2).

3. Results and discussion

The study was carried out for the base fluid (water) and nanofluid with ϕ = 1% and ϕ =4% considering both constant and temperature dependent properties to determine the heat transfer characteristics at three different Reynolds number viz. Re =500, 1000 and 1900. Figure 3 shows variation of temperature at the channel wall (T_w) for the nanofluid with ϕ =1% and ϕ =4% for both constant and variable property models at Re =500. Bulk mean temperature (T_m) variation of the nanofluid is also shown for variable property model. It was seen that both T_w and T_m increase along the channel and in case of the nanofluid with ϕ =4%, T_w and T_m were found comparatively less. Moreover, T_w also reduced slightly when variable properties were considered instead of fixed.

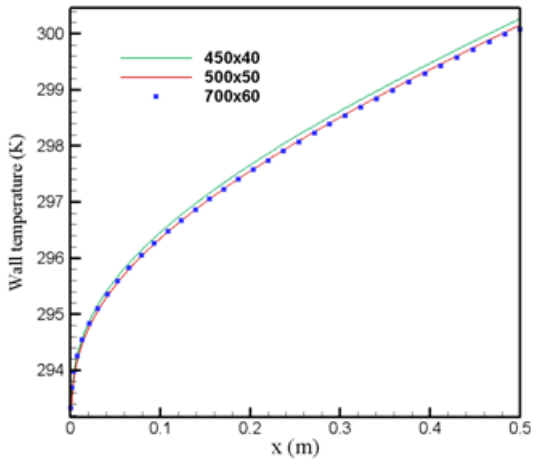

Figure 2. Wall Temperature at various grid size

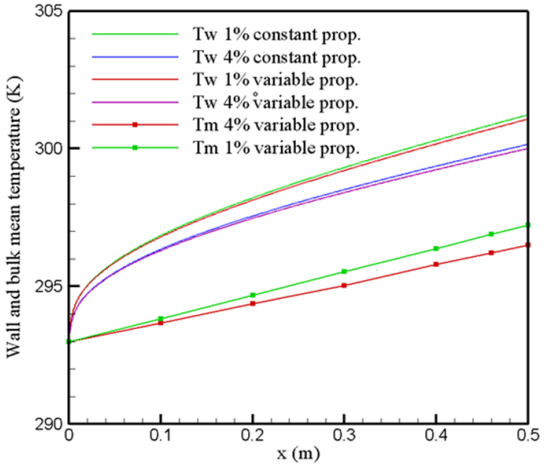

Figure 3. Wall temperature for constant and variable property models at Re=500 (grid size 500x50) and bulk mean temperature for variable property model with ϕ =1% and ϕ =4%

Variation of heat transfer coefficient along the microchannel is shown in Figure 4(a) for the base and nanofluid for both constant and variable property models. Heat transfer coefficient increased significantly in case of the nanofluid and it was also more for the nanofluid with ϕ =4% compared to that with ϕ =1%. Moreover, at a given ϕ, higher heat transfer coefficient was obtained with the variable property model. Figure 4(b) shows variation of heat transfer coefficient along the microchannel at various Reynolds numbers for the nanofluid with ϕ =4% (variable property). It was seen that heat transfer coefficient was more at higher Reynolds number. Heat transfer enhancement with nanofluids at higher particle concentration was reported in Refs. [1-7]. Thermal conductivity of the nanofluid is more compared to the base fluid which increases due to dispersion of nanosize solid particles in the base fluid.

This is depicted in Figure 5(a) which shows that thermal conductivity is more for the nanofluids and it is the highest for the nanofluid with ϕ=4%. Figure 5(b) shows that viscosity also increases significantly in case of the nanofluid and it was the maximum for the nanofluid with ϕ=4%. Further, it was seen that the viscosity of the nanofluid decreases along the channel while in case of the base fluid it shows an increasing trend.

Effect of higher viscosity of the nanofluid can be seen in Figures 6 (a) and 6 (b). It was found that the shear stress and skin friction coefficient was higher for the nanofluid compared to those of the base fluid and more so in case of the nanofluid with higher ϕ. Further, lower values of shear stress and skin friction coefficient were obtained in case of the variable property model. Bianco et al. [12] also found higher heat transfer coefficient and lower shear stress with the temperature dependent model. Figure 6 (c) shows that for the same outlet pressure of 1 atm., the pressure drop is more in case of the nanofluid and it increases with ϕ. However, the pressure drop was comparatively less for temperature dependent model. Heat transfer with finite temperature difference is an irreversible process, therefore, it is expected that maximum heat transfer should occur with minimum entropy generation. Figure 6 (d) shows that less entropy is generated when nanofluid is used and entropy decreases with increase in ϕ. Also, entropy generation is less in case of the variable property model.

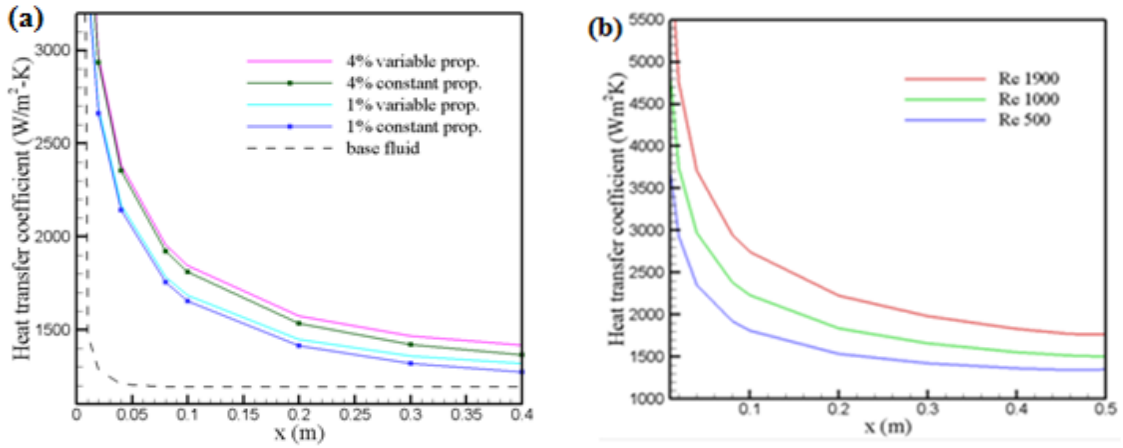

Figure 4. Heat transfer coefficient variation along the tube for (a) base and nanofluid with ϕ=1% and ϕ=4% at Re = 500 for both constant and variable property models (b) nanofluid with ϕ=4% at various Reynolds Numbers only for variable property model.

Variation of Nusselt number (Nu) along the microchannel for the base and naofluid with ϕ =1% and ϕ=4% is shown in Figure 7(a) for both the constant and variable property models. It was found that Nu decreases rapidly along the channel and assumes almost a constant value in case of the base fluid. In case of the nanofluid, however, it changes gradually and Nu value is more than that of the base fluid at all positions. Moreover, Nu was more for the nanofluid with ϕ=4% compared to that with ϕ=1%. Further, higher value of Nu was obtained with the variable property model. It was also observed that variation of heat transfer coefficient and Nu follow almost the same trend along the microchannel. Figure 7 (b) shows that Nu also increases with Re for both the base and nanofluid.

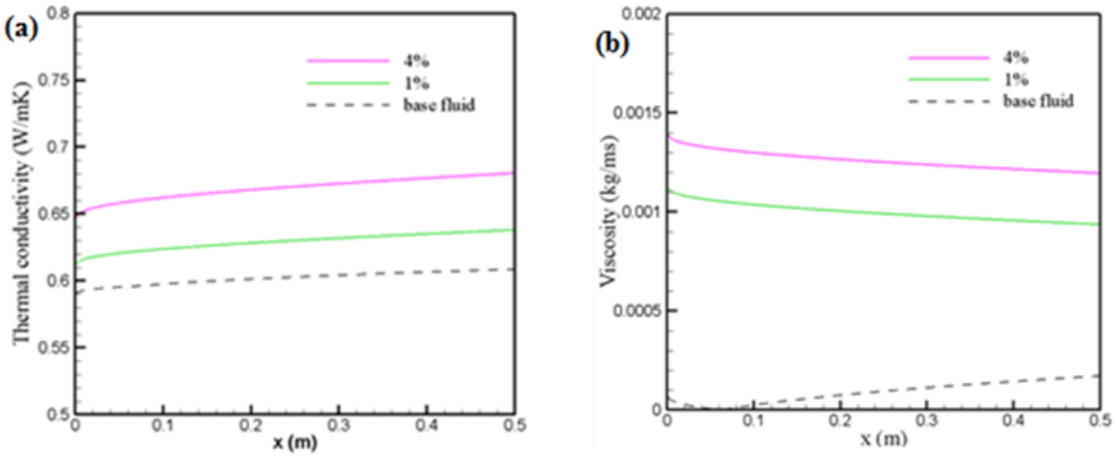

Figure 5. Variation of (a) thermal conductivity (b) viscosity for nanofluid with ϕ=1% and ϕ=4% along the microchannel wall at Re=500 for the variable property model

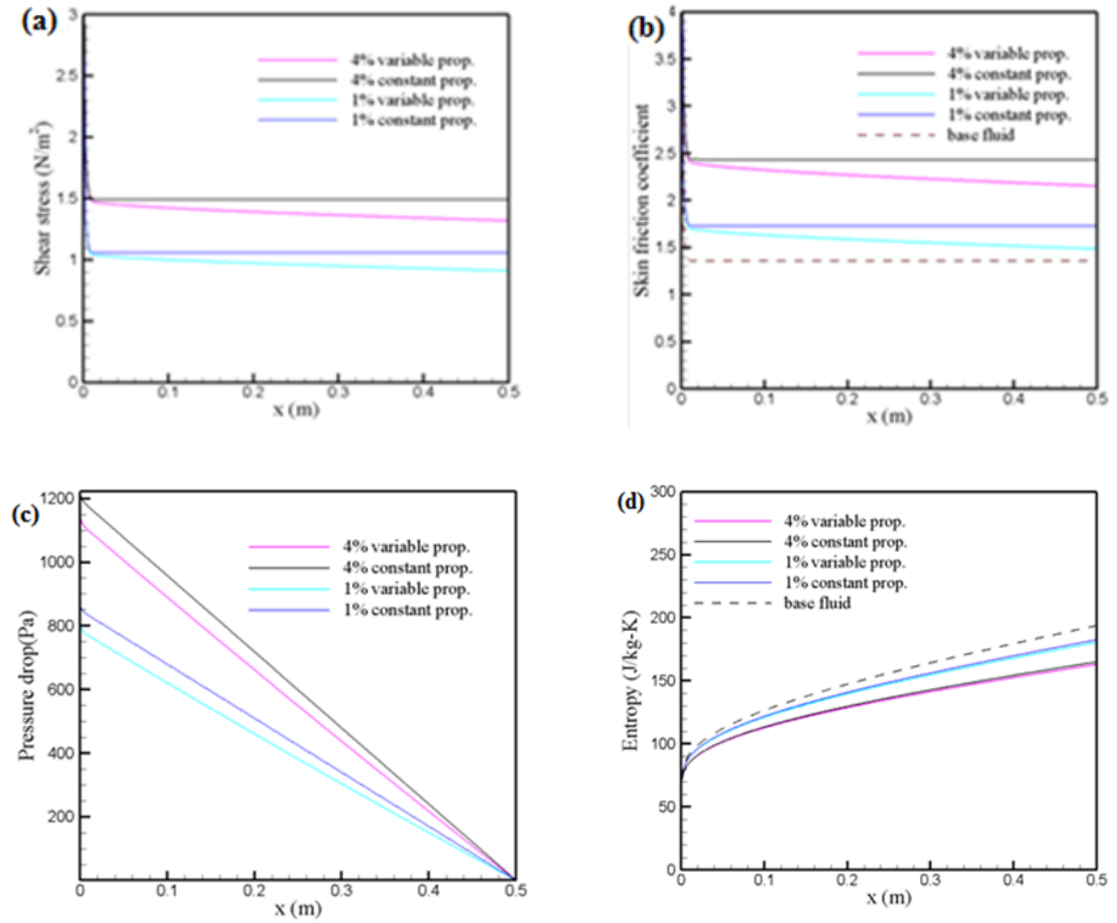

Figure 6. Variation of (a) entropy (b) pressure (c) shear stress (d) friction coefficient along the channel wall for base and nanofluid with ϕ=1% and ϕ=4% for both constant and variable property models at Re=500

4. Conclusions

In this study, laminar convective heat transfer characteristics of Al_2O_3 nanofluid in a circular microchannel with 1% and 4% volumetric concentrations is presented and compared with those of the

base fluid (water). Ansys Fluent is used to solve the problem using a discrete two phase model. Full details of heat transfer capability of nanofluid is provided along with comparison of results between base and nanofluid considering both constant and temperature dependent properties of nanofluid. Based on the results, the following conclusions were drawn.

1. Compared to the base fluid, heat transfer coefficient and Nusselt number were more for the nanofluid and these two parameters increased with ϕ and Re.
2. T_w and T_m were less in case of nanofluid and these were minimum for the nanofluid with ϕ=4%. T_w and T_m further reduced when temperature dependent model was considered.
3. Thermal conductivity of the nanofluid was more than the base fluid and it increased with ϕ, however viscosity also increased simultaneously.
4. Due to higher viscosity, the shear stress, friction and pressure drop were more in case of the nanofluid and values of these parameters increased with ϕ. However, the variable property model gave slightly better results.
5. Enhancement in heat transfer was achieved with the nanofluid with low entropy generation.

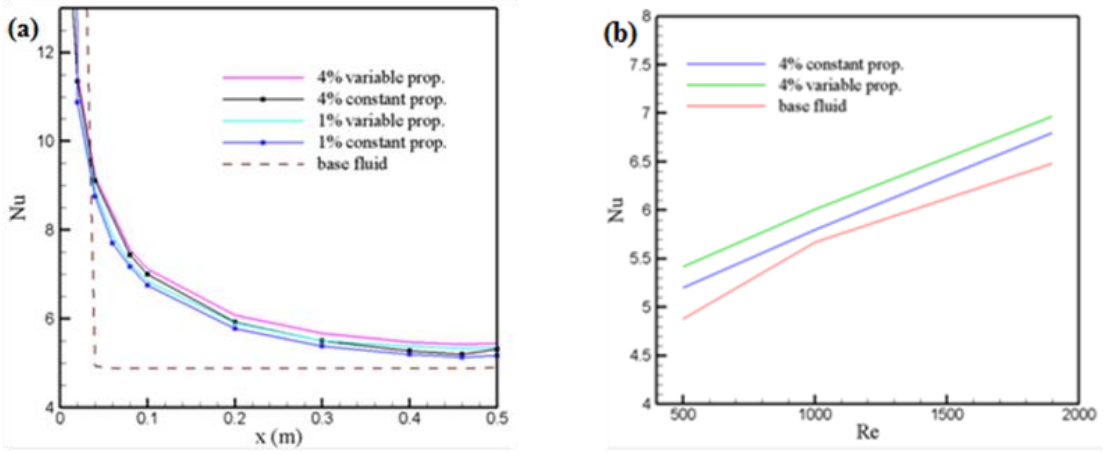

Figure 7. Nusselt number variation with (a) channel length for base and nanofluid with ϕ=1% and ϕ = 4% at Re=500 (b) Reynolds number for base and nanofluid with ϕ=4% for both constant and variable property models at the central location of the microchannel

REFERENCES:

[1] Wen D and Ding Y 2004 *Intl. J. of Heat and Mass Transfer* **47**(24) 5181-88
[2] Heris S Z, Esfahany M N and Etemad S G 2007 *Intl. J. of Heat and Fluid Flow* **28** 203-210
[3] Hojjat M, Etemad S G, Bagheri R, Thibault J 2011 *Intl. J. of Thermal Sciences* **50** 525-531
[4] Jung J Y, Oh H S, Kwak H Y 2009 *Intl. J. of Heat and Mass Transfer* **52** 466–472
[5] Lee J and Mudawar I 2007 *Intl. J. of Heat and Mass Transfer* **50**(3) 452 – 463
[6] Ho C J, Wei L C and Li Z W 2010 *Applied Thermal Engineering* **30** 96–103
[7] Kalteh M, Abbassi A, Saffar-Avval M, Frijns A, Darhuberd A and Harting 2012 *Applied Thermal Engg* **36** 260–268
[8] Maiga S E B, Palm S J, Nguyen C T, Roy G, Galanis N 2005 *Intl. J. of Heat and Fluid Flow* **26** (4) 530–546
[9] Chein R, Huang G 2005 *Applied Thermal Engineering* **25** 3104–14
[10] Jang S P, Choi S U S 2006 *Applied Thermal Engineering* **26** 2457–63
[11] Li J, Kleinstreuer C 2008 *Intl. J. of Heat and Fluid Flow* **29** 1221–32
[12] Bianco V, Chiacchio F, Manca O and Nardini S 2009 *Applied Thermal Engineering* **29**(17)3632–42
[13] Feng Y and Kleinstreuer C 2010 Nanofluid *Intl. J. of Heat and Mass Transfer* **53** 4619–28
[14] Kalteh M, Abbassi A, Saffar-Avval M, Harting J 2011 *Intl. J. of Heat and Fluid Flow* **32** 107–116

[15] Mashaei P R, Hosseinalipour S M. and Bahiraei M 2012 M. *J. of Applied Mathematics* Article ID 259284 1-18
[16] Hatami M and Ganji D D 2014 *Energy Conversion and Management* **78** 347–35
[17] Maiga S E B , Cong Tam N, Galanis N , Roy G, Mare T and Coqueux M 2006 *Intl. J. of Numerical Methods in Heat and Fluid Flow* **16** (3) 275–292
[18] Namburu P K, Das D K, Tanguturi K M and Vajjha R S 2009 Intl. J. of Thermal Sciences **48** 290–302
[19] Bianco V, Manca O and Nardini S 2011 *Intl.J. of Thermal Sciences* **50** 341-349
[20] Mohammeda H A, Bhaskarana G, Shuaiba N H and Saidurb R 2011 *Renewable and Sustainable Energy Reviews* **15** 1502–12
[21] Sohel M R, Saidur R, Faizul M, Sabri M , Kamalisarvestani M, Elias M M and Ijam 2013 A *Intl Communications in Heat and Mass Transfer* **42** 75–81
[22] Sohel M R, Saidur R, Hassan N H, Elias M M, Khaleduzzaman S S, Mahbubul I M 2013 *Intl. Communications in Heat and Mass Transfer* **46** 85–91
[23] Zhang H, Shao S, Xu H and Tian C 2013 *Applied Thermal Engineering* **61** 86-92
[24] ANSYS FLUENT 14.0 User's Guide, November 2011